**Ninth Canadian Conference on
Earthquake Engineering
Ottawa, Ontario, Canada
26-29 June 2007**

SEISMIC SHEAR FORCE DISTRIBUTION IN HIGH-RISE CONCRETE WALLS

P. Adebar[1] and B. R. Rad[2]

ABSTRACT

In high-rise buildings, concrete walls are tied together by rigid floor slabs at numerous levels, which significantly influences the seismic shear force distribution in walls. Nonlinear static analysis was used to examine how nonlinear behaviour of walls influences shear force distribution. Linear, bilinear and trilinear models were used to determine both flexural and shear rigidity of the walls. When the traditional bilinear (elastic–plastic) model is assumed for bending and strength is made proportional to stiffness, the shear forces in all walls increase proportionally until all walls yield at the same displacement. If a more realistic trilinear bending moment – curvature model is used, the shear force distribution becomes more complex, and the shear force will be higher in some walls than predicted by a linear analysis. When the influence of diagonal cracking is accounted for, the variation from linear analysis becomes greater. Additional shear deformations due to diagonal cracking also significantly influences the displacement when walls yield in flexure – a shorter length wall will actually yield in flexure at a smaller top wall displacement than a longer wall due to the increased shear deformations in the longer wall causing a local redistribution of shear forces near the base of the wall. While it is common practice to increase the shear demand proportional to any flexural over-strength using the results from linear analysis, nonlinear analysis suggests the increase in shear demand may be significantly larger than the increase in flexural capacity.

Introduction

In the design of high-rise concrete buildings, linear dynamic (response spectrum) analysis is normally used to determine the displacement demands on the overall structure, and the force demands on the individual components of the structure. The stiffness properties used in the analysis model must account for the presence of cracked regions of the concrete members. The effective flexural rigidity E_cI_e that is normally used for concrete walls is a portion of the gross section flexural rigidity E_cI_g of the walls. For simplicity, one reduction factor (e.g., 70%) is normally used for all elements in the structure. The effective shear rigidity of concrete walls is usually assumed to equal the gross section shear rigidity G_cA_v. That is, the effect of shear cracking is usually not accounted for. While these simple assumptions about effective member rigidities lead to reasonable estimates of overall structural displacement, such as the displacement at the top of concrete walls, they may result in poor estimates of shear force distribution between concrete walls.

[1]Professor, Dept. of Civil Engineering, University of British Columbia, Vancouver, Canada, V6T 1Z4
[2]Doctoral Candidate, Dept. of Civil Engineering, University of British Columbia, Vancouver, Canada, V6T 1Z4

In high-rise buildings, concrete walls are tied together over the height of the wall by rigid floor plates at every floor level. At the upper levels of the structure, the shear force distribution between walls depends primarily on the relative flexural rigidity of the walls. In the lower levels of the building, the shear force distribution depends more on the relative shear rigidity of the walls. Due to cracking of concrete and yielding of reinforcement, the shear and flexural rigidities of concrete walls will change as the wall is subjected to increasing shear and bending moments.

In this study, nonlinear analysis is used to make an accurate estimate of the shear force distribution in high-rise concrete walls. Experimentally calibrated models accounting for uncracked, cracked and post-yielding response of reinforced concrete were used to determine both flexure and shear rigidities of concrete walls. The results from the study confirm that the shear force distribution can be very different than suggested by linear analysis.

Nonlinear Models for Concrete Walls

Flexural Model

The response of a reinforced concrete element or structure to cyclic loading depends on the strain level reached in the previous cycles of loading as the stress-strain response of concrete in compression and tension, and the post-yielding stress-strain response of reinforcement is dependant on strain history. For a typical concrete wall, the effect of load-history on concrete compression response and reinforcement response can be ignored without significant error. On the other hand, the influence of strain history on concrete tension stresses is very significant for a typical concrete wall. Based on the results of large-scale reinforced concrete elements subjected to cyclic axial tension, Adebar and Ibrahim (2002) developed a simplified average stress - average strain relationship for concrete that they used to predict the bending moment - curvature response of concrete walls. The relationship reflects the fact that when concrete cracks, there is a small reduction in average concrete tensile stresses over the entire length of the element.

Adebar and Ibrahim (2002) proposed that the bending moment - curvature relationship for a typical high-rise concrete wall can be approximated by a simple trilinear relationship as shown in Fig. 1(a). The trilinear relationship is defined by four parameters: slope of the first straight line segment, which is assumed to be equal to the uncracked-section stiffness E_cI_g; slope of the second straight line segment, which is assumed to be equal to the cracked-section stiffness E_cI_{cr} when the section is subjected to zero axial load; bending moment M_l defining the intersection of the first and second linear segments, and; nominal flexural capacity of the section M_n. In order to validate the proposed trilinear bending moment - curvature model, Adebar et al. (n.d.) conducted a large-scale test on a slender concrete wall. A 12.5 m (41 ft) "high" concrete wall with a height-to-length ratio of 7.6 was constructed and tested in a horizontal position supported on sliding bearings. The wall had a flanged cross section, low percentages of vertical reinforcement (0.65% in the flanges and 0.25% in the web), and was subjected to a uniform axial compression that corresponds to $0.10\ f'_cA_g$ in addition to a reverse cyclic lateral point load applied at 11.33 m (37 ft) from the critical flexural section. Additional information about the test is given by Adebar and Ibrahim (2002), and a complete report is given by Adebar et al. (n.d.).

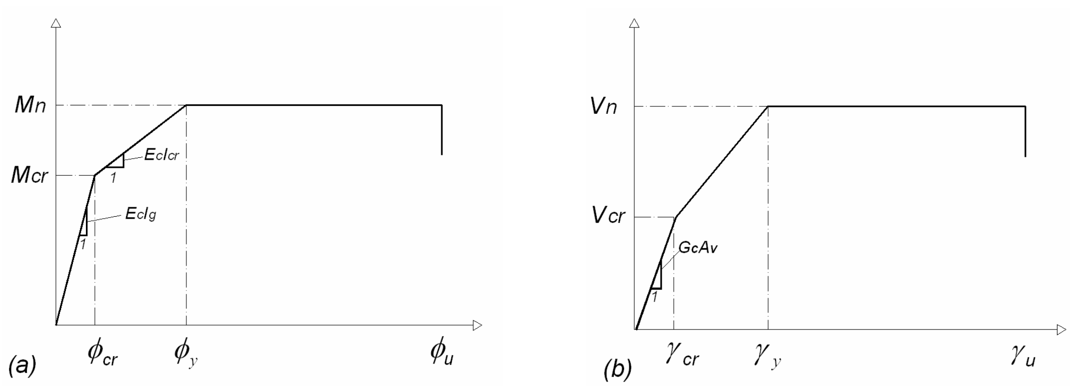

Figure 1. Nonlinear models for concrete walls: (a) Flexural model, (b) Shear model.

Shear Model

Based on large-scale experiments on reinforced concrete elements with uniform membrane stress and strains, Gerin and Adebar (2004) developed a simple tri-linear shear model for the nonlinear static analysis of concrete walls, and this is summarized in Fig. 1(b). Until diagonal cracking occurs at a shear force of V_{cr}, the slope of the shear force – shear strain curve is equal to the well-known shear rigidity of an uncracked concrete member G_cA_v. For simplicity, a straight line is assumed between the cracking point and the yield point, which is defined by the shear (yield) strength of the wall V_n and the shear strain at yielding γ_y.

$$V_n = v_y b_v d_v \tag{1}$$

where v_y is the shear stress at yield of the transverse reinforcement, b_v is the width of the wall and d_v is the effective shear depth of the wall, normally taken as 80% of the wall length (0.8 l_w).

Gerin and Adebar (2004) provided the following expression to estimate the shear strain at yielding:

$$\gamma_y = \frac{f_y}{E_s} + \frac{v_y - n}{\rho_v E_s} + \frac{4v_y}{E_c} \tag{2}$$

where f_y is the reinforcement yield stress, E_s is the reinforcement Modulus of Elasticity, n is the vertical axial compression stress P/A_g and ρ_v is the vertical reinforcement ratio.
The second term in Eq. (2) has the following limits:

$$0 \le \frac{v_y - n}{\rho_v E_s} \le \frac{f_y}{E_s} \tag{3}$$

The shear force to cause diagonal crack in a reinforced concrete wall can be estimated as:

$$V_{cr} = (f_{cr}\sqrt{1 + \frac{n}{f_{cr}}})b_v\, d_v \tag{4}$$

where f_{cr} is the uniaxial cracking strength of concrete:

$$f_{cr} = 0.33\sqrt{f'_c} \tag{5}$$

f'_c is the compression strength of concrete. The shear strain capacity of a wall γ_u depends on the shear stress ratio v_y / f'_c and the shear strain at yielding and is given by

$$\frac{\gamma_u}{\gamma_y} = 4 - 12\frac{v_y}{f'_c} \quad (6)$$

Note that as the shear stress ratio v_y / f'_c is increased, the shear strain ductility γ_u / γ_y reduces.

Example Problem

To investigate the issue of shear force distribution in high-rise concrete walls, a simple two-wall example as shown in Fig. 2 was used. In order to maximize the variation in shear force distribution, the two walls were purposely chosen to be very different. Wall W1 is a 9 m long wall with large transverse walls attached to the ends, i.e., a large flanged wall, while wall W2 is a rectangular wall that is 4.5 m long (half as long). Both walls have a "web" thickness of 0.75 m. Wall W1 represents a typical cantilever wall that is part of a building core. As both walls have the same overall height (81 m), wall W1 has half the height-to-length ratio of wall W2.

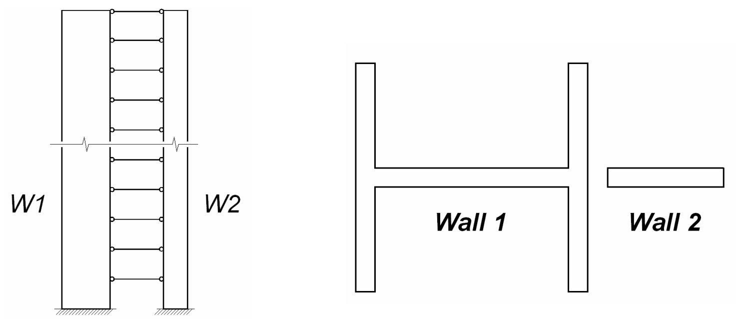

Figure 2. Simple two-wall example used in the current study.

In order to make it a realistic example, the strengths of the walls were determined the way it is done in practice, so the strengths are greater than or equal to the forces determined from a linear analysis. Response spectrum analysis (RSA) is the most common analysis method used in Canadian design practice to estimate the seismic demand on high-rise buildings. Thus this method was used to establish the relative strengths of the walls at the base of the building.

The simple model of the two interconnected walls is shown in Fig. 2. The walls are assumed to be connected together at each floor level by a rigid diaphragm. Thus the walls have the same horizontal displacement at each floor level. The diaphragm has an essentially infinite in-plane stiffness (hence modeled as rigid); but has a very low out-of-plane bending stiffness. For this reason, the ends of the rigid connections between the walls are assumed to be pin connected to the walls.

The RSA was conducted for the simple two-wall model by adjusting the uniform mass over the height of the 30-story building so that the fundamental period of the two-wall model was 3 sec., which is the typical value for a complete 30-story building. In other words, only the appropriate portion of the total mass of a complete 30-story building was applied to the two-wall model. The design spectrum that was used for the RSA was Vancouver site class C. To account for the effect of flexural cracking in the concrete walls, the effective flexural rigidity E_cI_e was taken as 70% of the uncracked flexural rigidity E_cI_g as is normally done in practice.

The shear forces and bending moment near the base of the walls determined from the RSA are as follows. The factored bending moments in walls W1 and wall W2 are M_{f1}= 1,125,500 kNm and M_{f2}=49,000 kNm, respectively. The factored shear force in wall W1 at level 1 V_{f1}= 34,000 kN, while the factored shear force in wall W2 at level 1 V_{f2}= 7,100 kN. Note that the ratio of M_{f1} to M_{f2} is 23.0, while the ratio of V_{f1} to V_{f2} at level 1 is 4.78. The ratio of (M_{f1} + M_{f2}) to (V_{f1} + V_{f2}) at the base is 28.5 m. Note that this value is much less than 2/3 × 81m= 54m due to the influence of higher modes.

The two walls were designed so that the resistances of the walls were about equal to the forces determined in the RSA. Both walls were assumed to be subjected to an axial compression equal to $0.1 f'_c A_g$ at the base of the walls, which for wall W1 is 114,750 kN, and W2 is 20,250 kN. To have the required flexural capacity at the base, wall W1 required about 2.5% vertical reinforcement in the transverse walls (flanges), and about 0.5% vertical reinforcement in the web. Wall W2 required 1% vertical reinforcement over 15% of the wall length at each end of the wall. To have adequate shear resistance, wall W1 required about 1% horizontal reinforcement at level 2, while wall W2 required about 0.3% horizontal reinforcement at level 1. The applied shear forces cause shear stress ratios v/f'_c of 0.1 in wall W1 at level 2, and $v/f'_c = 0.045$ in wall W2 at level 1.

Simplified Nonlinear Analysis

Nonlinear time history analysis is the most accurate procedure to assess the seismic performance of a concrete building; however the problem that is being discussed in the current paper – shear force distribution between walls – does not require such a complex analysis. Other aspects of nonlinear shear behaviour of concrete walls, such as the influence of higher modes on total shear demand on concrete walls in a building must be investigated using nonlinear dynamic analysis. These issues are being investigated as part of the current overall study on nonlinear shear response of high-rise concrete walls during earthquakes (Rajaee Rad, 2007); but are not discussed in the current paper. The relative shear force distribution between walls depends only on the nonlinear material behaviour of the concrete walls, and this can be investigated using nonlinear static analysis. The advantage of nonlinear static analysis is the simplicity and transparency of the analysis results which allows a complete understanding of the behaviour of the structure.

A uniformly distributed lateral load over a height of 62 m from the base (resultant lateral load at 31 m from the base) was used for the static analysis in order to result in a similar bending moment to shear force ratio at the base obtained from RSA. The resulting distribution of bending moments and shear forces over lower stories of the building are compared in Fig. 3.

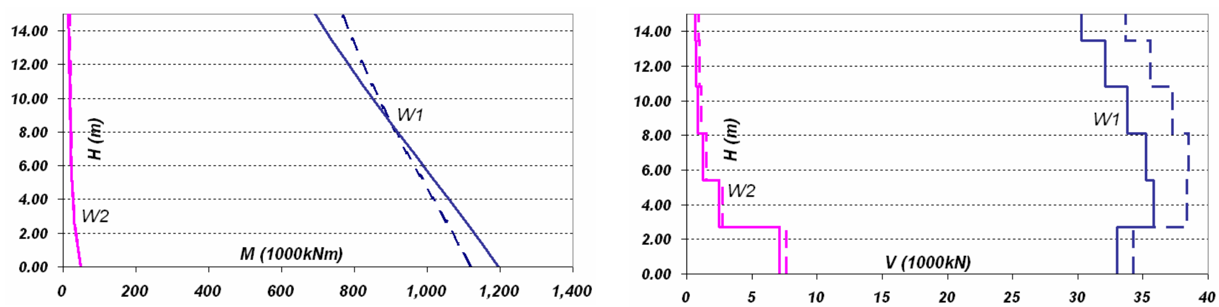

Figure 3. Comparison of bending moment and shear force distributions over lower floors from RSA (dashed lines) and linear static analysis (solid lines).

The shear forces and bending moments determined at base of walls from linear static analysis are summarized in Table 1. These are referred to as the factored forces, analogous to factored forces in design, and are used to normalize the plots in the results section. Note that the ratio of M_{f1} to M_{f2} is 24.4 while the ratio of V_{f1} to V_{f2} at level 1 and 2 are 4.64 and 14.5. The ratio of (M_{f1} + M_{f2}) to (V_{f1} + V_{f2}) at the base is 31 m.

Table 1. Summary of forces determined at base of walls from linear static analysis.

Parameter	Wall 1	Wall 2

Vf Level 2 (kN)	35,820	2,470
Vf Level 1 (kN)	33,000	7,100
Mf base (kNm)	1,195,500	49,000

The nonlinear static analyses were done using the trilinear models for flexure and shear described above. A summary of the nonlinear model parameters are given in Table 2. The nonlinear analyses were performed using program *SAP Nonlinear*. The flexural hinge length for walls was taken as one story height; in addition, sensitivity analysis was used to determine parameters such as event tolerance and the total number of analysis steps for the accuracy of results. The walls were assumed to be fixed at the base, and the structure below-grade was not included in the current study. The complex nonlinear behaviour in the below-grade portion of high-rise walls was recently examined in a separate study by the authors (Rajaee Rad, 2007).

Table 2. Nonlinear model parameters used for concrete walls in example.

Trilinear Flexural Model		
Wall	W1	W2
Level	1	
M_l (1000kNm)	424.9	22.47
$Ø_l$ (rad/km)	0.047	0.113
M_n (1000kNm)	1,195	49.00
$Ø_y$ (rad/km)	0.393	1.200
M_u (1000kNm)	1,198	49.13
$Ø_u$ (rad/km)	3.889	7.778

Trilinear Shear Model				
Wall	W1		W2	
Level	1	2	1	2
V_{cr} (1000kN)	23.75	23.75	6.39	2.22
γ_{cr} * 1000	0.315	0.315	0.170	0.059
V_n (1000kN)	33.00	35.80	7.10	2.47
γ_y * 1000	2.705	2.765	2.305	2.105
V_u (1000kN)	33.03	35.82	7.12	2.49
γ_u * 1000	7.505	7.385	8.005	8.035

Analysis Results

In order to understand how the nonlinear model influences the shear force distribution, nonlinear static analyses were performed on the two-wall example using different nonlinear models. Fig. 4 summarizes these different models. For flexure, either bilinear or trilinear models were used, while for shear, linear, bilinear and trilinear models were used. In the case of the linear and bilinear shear models, unlimited strength was assumed as shown in Fig. 4.

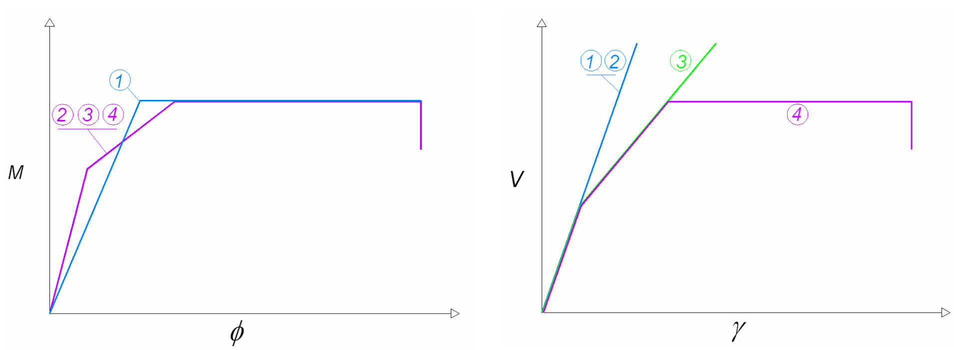

Figure 4. Shear and flexural models used in current investigation.

A standard format is used in the figures to summarize results. The dark blue lines in the figures indicate the results for the longer wall (W1), while the magenta lines indicate the results for the smaller wall (W2). Solid and dash lines represent the results for the first and second storey, respectively. Two separate plots are given to present the flexure and shear demands on walls. The shear and bending moment demands, shown on the vertical axes, have been normalized by the forces determined in the linear static analysis and summarized in Table 1. In all cases, the horizontal axis is the displacement at top of walls. A summary of the important points in the response is given in Table 3.

Fig. 5 summarizes the results from Model 1 in which the walls are assumed to respond linearly in shear and bilinearly (elastic-perfectly plastic) in flexure. The analysis was performed using $0.7E_cI_g$ for effective flexural rigidity of the walls as was done to determine the factored forces given in Table 1. Since the stiffnesses are proportional to the strengths, the walls yield at base at exactly the same time. This simple response is what most engineers assume is happening in concrete walls. Note that while the shear strengths of the walls are assumed to be unlimited, the shear demand is limited by flexural yielding at the base. The shear force demand is limited exactly to the shear force determined in the linear analysis.

The results from Model 2 are shown in Fig. 6. The shear model is unchanged (linear with unlimited strength), while the flexural model is now trilinear. The initial flexural rigidity is increased to the uncracked section rigidity E_cI_g of the wall, but a significant reduction in flexural rigidity occurs after cracking (see Fig. 4). The reduction in flexural rigidity occurs at a curvature Φ_l in wall W1 that is less than half the Φ_l of wall W2 (0.047 versus 0.113; see Table 2).

Table 3: Summary of important points in analysis results.

Fig.5		
Disp	State*	Level
0.380	F-Y-1	1
0.380	F-Y-2	1
Fig.6		
Disp	State*	Level
0.097	F-C-1	1
0.118	F-C-2	1
0.118	F-C-1	2
0.219	F-C-2	2
0.385	F-Y-1	1
0.441	F-Y-2	1

Fig.7		
Disp	State*	Level
0.097	F-C-1	1
0.118	F-C-1	2
0.118	F-C-2	1
0.218	S-C-1	2
0.218	F-C-2	2
0.227	S-C-1	1
0.337	F-Y-2	1
0.428	F-Y-1	1
Fig.8		
Disp	State*	Level
0.10	F-C-1	1
0.12	F-C-2	1
0.12	F-C-1	2

Fig.8 Continue		
Disp	State*	Level
0.22	S-C-1	1
0.22	S-C-1	2
0.22	F-C-2	2
0.24	S-C-2	2
0.31	S-C-2	1
0.35	F-Y-2	1
0.42	S-Y-1	1
0.42	S-Y-1	2
0.44	S-Y-2	2
0.45	F-Y-1	1
0.47	S-Y-2	1
0.50	S-F-1	2
0.50	S-F-2	2

Fig.9		
Disp	State*	Level
0.380	F-C-1	1
0.391	F-C-2	1
Fig.10		
Disp	State*	Level
0.097	F-C-1	1
0.118	F-C-2	1
0.118	F-C-1	2
0.218	S-C-1	2
0.218	F-C-2	2
0.227	S-C-1	1
0.331	S-C-2	1
0.373	F-Y-2	1
0.423	F-Y-1	1

* State: F= Flexural, S= Shear, C= Cracked, Y= Yielded, F=Failure, 1= Wall 1, 2= Wall 2.

As a result, flexural cracking occurs at the base of wall W1 first at a top wall displacement of 0.1 m. At that point, the shear begins to redistribute so that wall W2 picks up an increasing amount of the total shear. Flexural cracking at the base of wall W2 occurs at a top displacement of 0.12 m, and at that point the shear force in wall W2 at level 1 (solid magenta line) begins to drop. Flexural cracking also occurs at that point in wall W1, level 2, so the drop in shear in wall W2 at level 2 is delayed until a top displacement of 0.22 m when wall W2 cracks at that level. At a displacement of 0.27 m, wall W2 cracks at level 3 causing the shear in wall W2 level 2 to start increasing again. Yielding of wall W1 occurs at a top displacement of 0.39 m, while yielding of wall W2 does not occur until a top displacement of 0.44 m. Note that according to the trilinear bending moment – curvature models that were assumed, yielding of wall W2 occurs at a curvature Φ_y that is about three times the yield curvature Φ_y of wall W1 (1.20 versus 0.39; see Table 2). Due to the large reduction in flexural rigidity at cracking in wall W2, wall W1 is subjected to a shear force that is about 10% larger than what is estimated by a linear analysis.

Fig. 7 presents the results from Model 3, which is the same as Model 2 (Fig. 6) except that the reduction in shear rigidity that occurs at shear cracking is now included. The initial response in Fig. 7 is the same as the response in Fig. 6. At a top displacement of 0.22 m, shear cracking occurs in wall W1 at level 2 where the shear is largest in that wall. This causes a very dramatic increase in the shear force in wall W2 at level 1 and particularly at level 2. As a result, the shear demand in wall W2 at level 2 increases 40% over what is predicted by a linear analysis. Due to the shear deformations of wall W1 and the resulting shear force redistribution, wall W2 now yields at a top displacement of 0.34 m, while wall W1 yields at a top displacement of 0.43 m. That is, the wall with a yield curvature that is three times larger actually yields first. This is a very significant result.

Fig. 8 presents the results from Model 4 in which shear yielding is included. The shear strengths of the walls were set equal to the shear demands determined from a linear analysis and summarized in Table 1. Yielding of the horizontal reinforcement in the wall, i.e., shear yielding of the wall, occurs in wall W1 at both level 1 and level 2 at a top displacement of 0.42 m (see Table 3). At a slightly larger displacement (0.44 m), shear yielding occurs in wall W2 at level 2, and then at 0.47 m, shear yielding occurs in wall W2 at level 1. Yielding in the walls occurs because the nonlinear behaviour of the walls causes redistribution and the shear demand exceeds the shear capacity. Shear failure occurs at level 2 in walls W1 and W2 at a top displacement of 0.5 m.

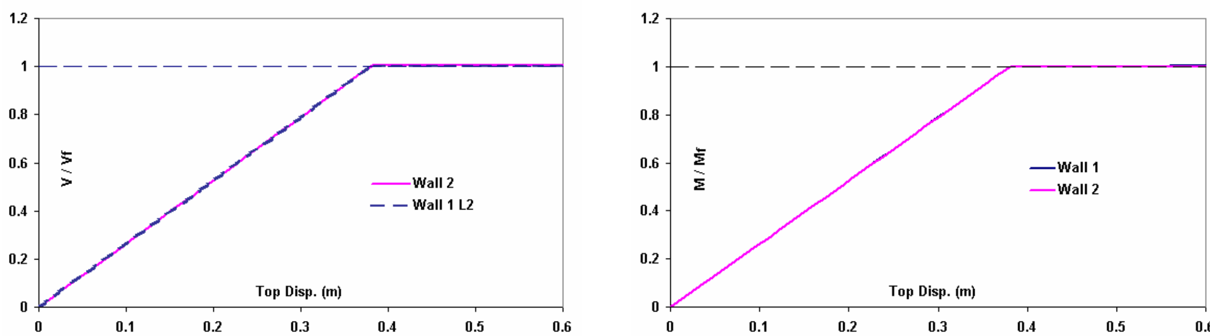

Figure 5. Normalized shear and flexure demand predicted by Model 1.

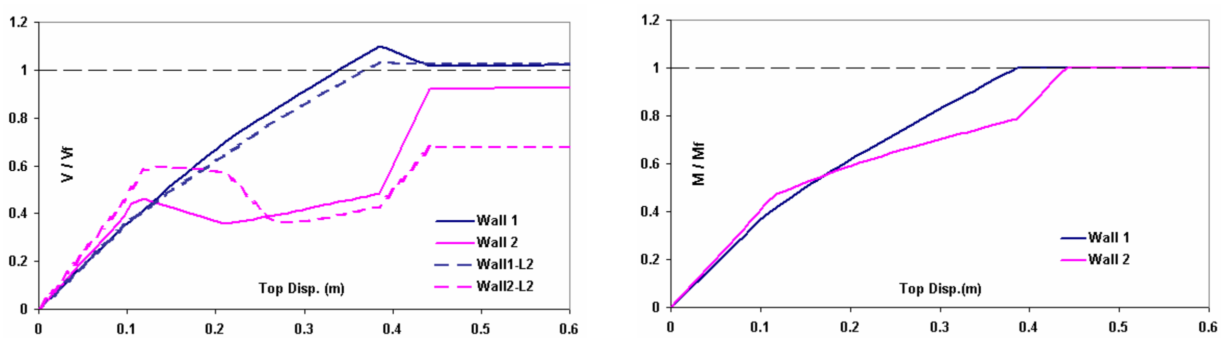

Figure 6. Normalized shear and flexure demand predicted by Model 2.

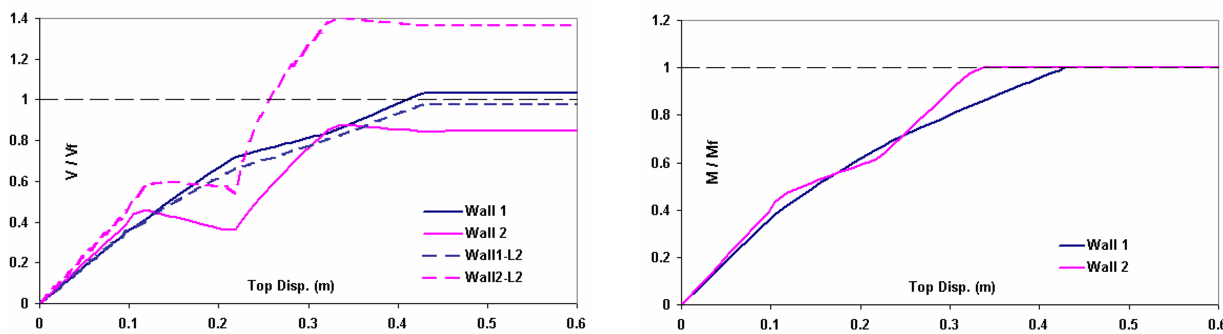

Figure 7. Normalized shear and flexure demand predicted by Model 3.

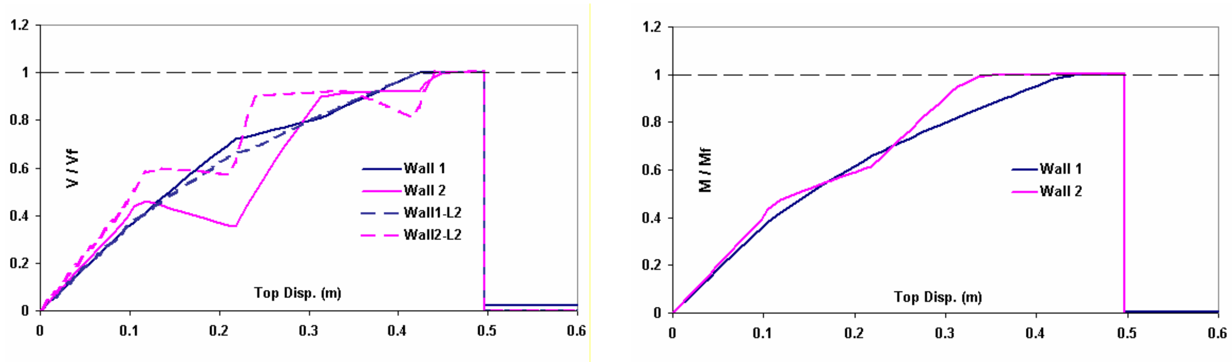

Figure 8. Normalized shear and flexure demand predicted by Model 4.

The influence of a 10% increase in the flexural capacity of wall W2 over the linear flexural demand is investigated in Figs. 9 and 10. Fig. 9 presents the results from Model 1 (bilinear flexure and linear shear), and thus should be compared with the results in Fig. 5. Model 1 predicts about a 20% increase in shear demand at the first level and about a 15% increase in shear demand at the second level due to the 10% increase in flexural capacity. Fig. 10 presents the results from Model 3 (trilinear flexure and bilinear shear), and should be compared with the results in Fig. 7. Model 3 predicts also about a 20% increase in shear demand at the second level (V = 1.7 V_f in Fig. 10 versus V = 1.4 V_f in Fig. 7) due to a 10% increase in flexural capacity.

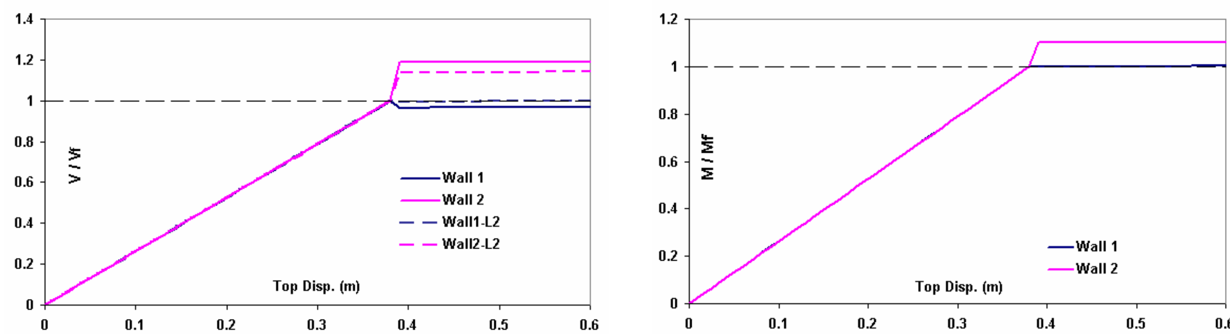

Figure 9. Influence of 10% flexural overstrength of W2 according to Model 1.

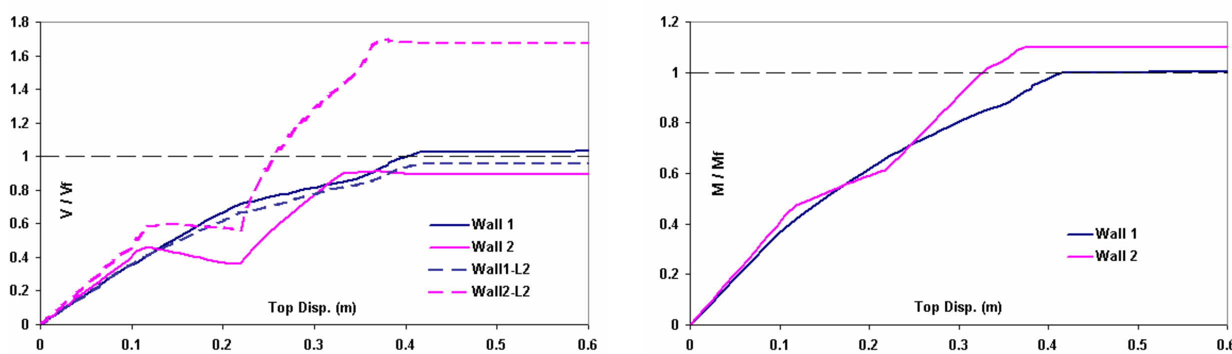

Figure 10. Influence of 10% flexural overstrength of W2 according to Model 3.

Conclusions

The simple model that is normally used for concrete shear walls is bilinear (elastic–plastic) in bending, and linear until brittle failure in shear. If the strengths of the walls are proportional to the stiffness, i.e., proportional to the results from a linear analysis, this model predicts a simple response where the shear forces in all walls increase proportionally until all walls yield at the same displacement. The actual bending moment – curvature response of a concrete shear wall is close to trilinear (Adebar and Ibrahim 2002), due to the significant reduction in flexural rigidity that occurs after flexural cracking. When this is accounted for, the shear distribution in concrete shear walls becomes much more complicated (see Fig. 6). The shear force distribution changes significantly as the walls crack at various levels. As a result of this redistribution, the shear force will be higher in some walls and lower in other walls than predicted by a linear analysis. This higher demand requires higher shear strength to avoid a shear failure. When diagonal cracks form in concrete shear walls, the shear rigidity reduces significantly. Gerin and Adebar (2004) have presented a simple trilinear model to account for diagonal cracking in concrete shear walls. When this is accounted for, very significant changes occur to the shear force distribution. For example, in Fig. 7, a 40% increase in the shear force in wall W2 at level 2 was observed.

The other very significant consequence of accounting for diagonal cracking is the change to the displacement at which the walls yield in flexure. This can best be seen by comparing the flexural results (right-hand side) of Figs. 6 and 7. When the shear deformations due to diagonal cracking are ignored, the predicted yield displacements of wall W1 and W2 are 0.39 m and 0.44 m, respectively. When the additional shear deformations are included, the yield displacement of wall W1 (longer wall) increases to 0.43 m, while the yield displacement of wall W2 actually reduces to 0.34 m. The reason is the longer wall (W1) has much more shear deformation than wall W2 near the base of the structure, and therefore significant shear is transferred to wall W2 locally at the base of the wall. These high shear forces near the base (as opposed to shear applied near the top of the wall) cause the wall to yield at a smaller displacement. The important observation that accounting for shear deformations from diagonal cracking results in a shorter length wall yielding prior to a longer wall (both walls have the same height) was subsequently confirmed by Bohl and Adebar (2007) using nonlinear finite element analysis of cantilever concrete shear walls.

The fact that a shorter length wall yields prior to a longer wall is very significant as it has been suggested by others (e.g., Paulay 2001) that cantilever shear walls can be designed by assuming the yield displacement is proportional to wall length. Adebar et al. (2005) have demonstrated that when high-rise cantilever walls are tied together by rigid floor slabs at numerous levels, all walls yield at the same displacement (the system yield displacement) regardless of wall length. The results presented in this paper demonstrate that when diagonal cracking is included in the analysis, all walls do not necessarily yield at the same displacement due to the differing shear deformations; however the results do reaffirm that the yield displacement of the walls is a system phenomenon and is not proportional to wall length.

It is common practice to increase the shear demand proportional to any flexural over-strength using the results from linear analysis. See for example Mitchell and Paultre (2006). The results from the nonlinear analysis summarized in Figs. 9 and 10 suggest that this may be unconservative as the increase in shear demand can be significantly larger than the increase in flexural capacity.

References

Adebar, P., and A.M.M. Ibrahim, 2002. Simple Non-linear Flexural Stiffness Model for Concrete Shear Walls, Earthquake Spectra, EERI, 18(3), 407-426.

Adebar, P., Ibrahim, A.M.M., and Bryson, M. n.d. Test of a High-Rise Shear Wall: Effective Stiffness for Seismic Analysis, *ACI Structural Journal*. In press (to be published in 2007).

Adebar, P., Mutrie, J., and DeVall, R., 2005. Ductility of Concrete Walls: The Canadian Seismic Design Provisions 1984 to 2004, *Canadian Journal of Civil Engineering*, 32: 1124 – 1137.

Bohl, A. and Adebar P., 2007. Plastic Hinge Length in High-Rise Concrete Shear Walls, 9th Canadian Conference on Earthquake Engineering, Ottawa, June.

Gerin, M., and Adebar, P. 2004. Accounting for Shear in Seismic Analysis of Concrete Structures," 13th

World Conf, on Earthquake Eng., Vancouver, Aug. 2004, CD Rom Paper No. 1747, 13 pp.

Mitchell, D., and Paultre, P., 2006. Chapter 21 Seismic Design, Concrete Design Handbook, 3rd edition, Cement Association of Canada, pp. 125 -156.

Paulay, T. 2001. “Seismic response of structural walls: recent developments, Canadian Journal of Civil Engineering, Vol. 28, pp. 922-937.

Rajaee Rad, B., 2007. “Seismic shear demand on high-rise structural walls”, Ph.D. thesis, Department of Civil Engineering, The University of British Columbia, Canada. (in press).